

# Mössbauer Study of Diffusion in Liquids: Dispersed Fe<sup>2+</sup> in Glycerol and Aqueous-Glycerol Solutions\*

A. Abras<sup>†</sup> and J. G. Mullen

*Physics Department, Purdue University, West Lafayette, Indiana 47907*

(Received 5 July 1972)

Mössbauer parameters, diffusion constants, and coefficients of viscosity for Fe<sup>2+</sup> ions, dissolved from FeCl<sub>2</sub>·4H<sub>2</sub>O, in nominally dry glycerol, glycerol-5-wt% water, and glycerol-10-wt% water have been measured. The broadening of the Mössbauer line is observed to have a complicated temperature dependence, which we explain by assuming two mechanisms of diffusion. At low temperatures we postulate that diffusion is via a jumping process described by an Arrhenius relation, while at high temperatures, diffusion is via a gaslike motion obeying the Einstein-Stokes and Litovitz relations. A quantitative fit to the observed line broadening is excellent. A very rapid falloff in the quadrupole splitting and the logarithm of the recoil-free fraction is observed in the temperature region where diffusive broadening is measurable; this falloff is proportional to the observed broadening, with two distinct proportionality constants for the low- and high-temperature regions. These observations are explained by a phenomenological theory due to Jensen and by postulating that the average electric field gradient at the iron nucleus reduces in proportion with the iron diffusivity.

## I. INTRODUCTION

Singwi and Sjölander<sup>1</sup> extended the self-correlation formalism, proposed by Van Hove,<sup>2</sup> to the resonance absorption of the  $\gamma$  rays. Through a self-correlation function  $G_s(\vec{r}, t)$ , which may be defined as the probability that an atom will undergo a displacement  $\vec{r}$  in a time interval  $t$ , they showed that recoil-free fraction, spectrum line shape, and linewidth for an emitter, or absorber, could be related to the dynamics of the emitting or absorbing nuclei. By assuming that a particle alternately performs an oscillatory motion for a mean time  $\tau_0$ , and then diffuses by continuous translation for a mean time  $\tau_1$ , Singwi and Sjölander explicitly treat two limiting cases,  $\tau_1 \gg \tau_0$  and  $\tau_0 \gg \tau_1$ . One can summarize the results predicted for a nucleus moving in two idealized limits as follows.

(i) A continuous-diffusion model, or Brownian motion (as in a liquid) when  $\tau_1 \gg \tau_0$ . This leads to a broadening of the Mössbauer spectrum with no change in the basic Lorentzian line shape and no reduction in over-all recoil-free fraction from that expected in the absence of diffusion. The broadening (in energy units) is given by  $\Delta\epsilon = 2\hbar\bar{k}^2D$ , where  $\hbar$  is Planck's constant divided by  $2\pi$ ,  $\bar{k}$  is the wave vector of the  $\gamma$  ray, and  $D$  is the diffusion coefficient.

(ii) A sudden-jump approximation analogous to solid-state diffusion when  $\tau_0 \gg \tau_1$ . If the nucleus jumps instantaneously between fixed sites, with no correlation between one jump and the next, a broadening of the spectrum is predicted. The theoretical line shape is shown to remain Lorentzian and the recoil-free fraction to follow the usual Debye-Waller temperature dependence.

A convenient way to characterize both of these limits has been suggested<sup>3</sup> through the relation

$$\Delta\epsilon/\Gamma_N = \sigma(\bar{k}^2\tau_N)D, \quad (1)$$

where  $\Delta\epsilon$  is the incremental broadening of the Mössbauer line,  $\Gamma_N$  is the natural width of the nuclear level ( $\hbar/\tau_N$ ),  $\sigma$  is a dimensionless constant [equal to 2 for case (i) and about 0.04 for uncorrelated-jump diffusion with a jump distance of 3 Å], and  $\tau_N$  is the mean nuclear lifetime of the Mössbauer isomeric transition.

The first reported measurements of diffusion effects by the Mössbauer technique was published by Bunbury *et al.*<sup>4</sup> and Craig and Sutin<sup>5</sup> studying the Fe<sup>57</sup> resonance in glycerol, which in the liquid phase is very viscous at low temperature. The data of Bunbury *et al.* were explained by an assumption of both continuous and sudden-jump diffusivity effects in the ratio of about 1:3, whereas Craig and Sutin were able to explain their results purely in terms of a continuous-diffusion model, where the ratio of temperature to viscosity was calculated from extrapolated values of the viscosity, and the Einstein-Stokes relation was assumed to relate diffusivity and viscosity. A number of features in the two experiments differed and may have served as the reason for the discrepancies. Craig's experiment used Co<sup>57</sup> in glycerol and gave a minimum linewidth much greater than expected from the uncertainty relation. Also, possible complications associated with  $K$  capture prior to the emission of the 14.4-keV line could not be ruled out.

Bunbury *et al.*, on the other hand, were looking at Fe<sup>3+</sup> resonances with large admixtures of Fe<sup>2+</sup> owing to difficulties in chemical processing. The

$\text{Fe}^{3+}$  resonance is complicated to analyze because the quadrupole splitting of the  $\text{Fe}^{57}$  level is of the same order as that of the expected minimum linewidth at low temperatures. This is a serious complication as a temperature-dependent quadrupole splitting would make it uncertain what reference linewidth should be subtracted from the observed linewidths to obtain the incremental broadening. To get around these difficulties and resolve the experimental questions we tried looking at the Mössbauer effect in many liquids<sup>6</sup> and found that  $\text{Fe}^{2+}$  in glycerol was the most satisfactory in that it gave a minimum linewidth of about 0.4 mm/sec, only twice that of the ideal linewidth predicted by the uncertainty relation.

Another motivation for the present experiment had to do with a desire to quantitatively compare the Singwi-Sjölander theory with experiment in the continuous-diffusion limit. An earlier measurement by Knauer and Mullen<sup>3</sup> had shown that for solid-state diffusion of iron in copper and gold, there is a serious quantitative discrepancy between the experimental line broadening and that predicted by the jump model of the Singwi-Sjölander theory. Their suggestion that correlation is responsible for the discrepancy has led to a more general formulation of the theory in the sudden-jump limit.<sup>7,8</sup> We wanted to see what kind of quantitative comparison could be made with the Singwi-Sjölander theory in the continuous-diffusion limit. Also, to check whether the measured broadening of our Mössbauer spectra depends on viscosity as found by Craig and Sutin,<sup>5</sup> we varied the viscosity of our glycerol samples by dilution with water, as well as by systematically changing the temperature.

Champeney and Woodhams<sup>9</sup> have also investigated molecular motion in liquids using a scattering technique. They were not able to get a satisfactory comparison with several models which have been proposed for liquid diffusion. In order to try to resolve these difficulties, we felt that more precise measurements would be required with much more data to check on errors and reproducibility. Also, we have measured the viscosity and classical diffusivity of our specimens directly to allow a comparison which would not permit sample variations to confuse the interpretation.

Recently Jensen<sup>10</sup> has studied liquid diffusion using the Mössbauer effect for  $\text{Fe}^{57}$  in propane-(1,3)-diol. Similar to the earlier studies of Knauer and Mullen,<sup>3</sup> he found a rapid falloff in the recoil-free fraction in the region where diffusion broadening occurred, which he explained in terms of a phenomenological theory, predicting a line broadening proportional to the logarithm of the recoil-free fraction. The recoil-free fraction has also been measured in the present study and a comparison with Jensen's description is given.

## II. EXPERIMENTAL TECHNIQUES

### A. Sample Preparation

In the preparation of the samples, the cleanest crystals of commercial ferrous chloride,  $\text{FeCl}_2 \cdot 4\text{H}_2\text{O}$  (Baker analyzed reagent and Mallick-rod analytical reagent), were selected. These crystals were dissolved in glycerol (99.2% dry-impurity contents, other than  $\text{H}_2\text{O}$ , had been analyzed at less than 0.001%) in the proportion of 1 g of the salt for 15 g of the solvent. This particular composition was chosen to get a desirable concentration of iron for the Mössbauer measurements. In terms of molarity, 1 g of salt per 15 g of solvent corresponds to about 0.42M at room temperature. Because of the high viscosity of the glycerol and low solubility of ferrous chloride in glycerol at room temperature, a flask of the mixture was kept in a water bath at 70 °C for about one week in order to have the salt completely dissolved. During this process, small amounts of hydrochloric acid (reagent A. C. S.) were added which made the pH of the solution between about 2 and 3. The reason for adding acid was that previous preparation of similar solutions showed possible precipitation or oxidation within approximately one week after the preparation. Initially, a fresh solution, which did not have HCl added, was faint green and showed a sharp doublet characteristic of  $\text{Fe}^{2+}$ . Aging would take place, however, as evidenced by an increasing transparency with time, and the Mössbauer spectra evolved a complex pattern superposed onto the usual  $\text{Fe}^{2+}$  doublet. It was found that this aging effect could be eliminated by adding a small quantity of hydrochloric acid (pH  $\approx$  2.5), a familiar technique for dispersing colloids.

Approximately 2 liter of the ferrous-chloride-glycerol solution was prepared, from which two other solutions were obtained by adding 5- and 10-wt% distilled and deionized water, respectively, to the dry-sample solution. It is convenient to label the three solutions as follows: Solution A, nominally "dry," is the solution with no water added, although it may contain 3-4-wt% water; solution B is solution A + 5-wt% water; and solution C is solution A + 10-wt% water.

In these experiments several samples were prepared, particularly of type A, to verify the reproducibility of the data. In samples where tracer diffusion measurements were made, using  $\text{Fe}^{59}\text{Cl}_2$ , the Mössbauer spectra agreed very well with the nonradioactive samples. Because several samples were made, and because we also measured the diffusivity and viscosity of our samples, natural iron was used throughout instead of enriched  $\text{Fe}^{57}$ . Although our weight concentration was about 7% of the solvent weight, we only observed  $\sim$ 15% increase in viscosity for our samples compared to those

with no salt added.

The sample A which we nominally label as dry may have had 3–4% water. This resulted from the fact that even the driest vacuum-pumped glycerol, used as a starting solvent has about 1-wt% water, while the salt added  $\text{FeCl}_2 \cdot 4\text{H}_2\text{O}$  contributed another 2- or 3-wt% water. Weighing the sample before and after heating to dissolve the salt indicated that additional water was not acquired during this operation.

To verify that the dissolved salts dispersed in glycerol, and did not form colloids, two samples were prepared by dissolving different salts in glycerol. Ferrous chloride and ferrous ammonium sulfate were dissolved in separate glycerol solutions, and the temperature dependence of the Mössbauer parameters (linewidth, quadrupole splitting, and recoil-free fraction) were found to be identical within the experimental errors, indicating that the salts were indeed dispersed.<sup>6,11</sup>

The stability of the solutions regarding possible crystallization was checked by taking subsequent Mössbauer runs over intervals of months. The water content in the solutions was monitored periodically by measuring the specific gravity.

Rough thermal analyses were carried out and they showed that our salt-carrying samples, like pure glycerol, are liquid-glass substances, with a glass-liquid transition temperature of approximately 185, 175, and 170 °K for solutions A, B, and C, respectively. The absence of sharp changes in the derivative of the warm-up curve supports the expected results that our samples did not have any crystalline phases in the temperature interval investigated.

The samples used in the Mössbauer experiments were encapsulated and set up according to the following procedure. The sample holders consisted of annular Plexiglas rings which were sealed with thin Plexiglas disks. Two calibrated copper-constantine thermocouples, protected by thin Pyrex tubing, were permanently sealed inside of the holders to monitor the temperature at the center and at the edge of a sample. To improve physical contact between thermocouples and solution, a small amount of silicone grease was introduced in the tubing. The holders were filled by injecting solutions A, B, or C with hypodermic needles through a small hole in the side of the ring, which was then sealed with epoxy. By means of this technique all Mössbauer samples were completely air tight preserving the initial characteristics of the solutions. Mössbauer spectra taken with these samples gave very reproducible results independent of aging or temperature cycling.

To detect any possible convective current due to thermal gradients, some special samples were prepared following the procedure described above,

except for the inclusion of either a porous foam disk or plastic powder inside the Plexiglas walls. Placing the sample in such a fine-grained structure would guarantee that macroscopic hydrodynamic motion of the solution could not take place. The plastic powder used was the organic compound methyl methacrylate (polymerized), with particles of about 100–600  $\mu\text{m}$  in diameter. The comparison between broadening of samples with and without foam (or plastic powder) were identical within the experimental errors. This showed that no convective current was present, and in subsequent experiments no foam or plastic powder was used.

#### B. Method of Measurement

The Mössbauer data were taken on a constant-velocity spectrometer described in the literature.<sup>12</sup> Sample temperature was measured in the center and edge of the disc-shaped sample. The temperature of the samples was controlled by means of a heater attached to the bottom of a Dewar with the aid of a commercially available temperature controller.<sup>6</sup> Errors in the measured temperature were believed to be within about 1 °K.

The viscosity of the sample solutions and pure glycerol was measured using calibrated Cannon-Fenske viscometers, supplied and certified by United Scientific Co. The method used is a standard procedure using inexpensive equipment. It deals with the determination of the kinematic viscosity, by measuring the time of flow of a fixed volume of liquid at a given temperature through a calibrated and shaped glass tubing. The kinematic viscosity (in centistokes) is given by the product of the flow time (in second) times the viscometer constant (in centistokes/sec). The dynamical viscosity or absolute viscosity (in cP) is given by the product of the kinematic viscosity (in centistokes) times the density (in  $\text{g}/\text{m}^3$ ) at the temperature of the experiment.

Diffusivity of  $\text{Fe}^{59}$  was measured directly in our experiments by a tracer-capillary technique described in detail by others.<sup>13–15</sup> Tracer quantities of  $\text{Fe}^{59}$  were added in the  $\text{Fe}^{2+}$  charge state and did not materially alter the total iron content in our samples, as was proven by showing that the  $\text{Fe}^{57}$  Mössbauer spectra were unchanged. The optimum capillary diameter was about 0.55 mm, with a stirring rate of 1 rpm within the nonradioactive bath solution external to the capillaries. The depletion in the  $\text{Fe}^{59}$  content in the capillary was measured with a standard 3×3-in. NaI(Tl) crystal and associated scintillation electronics.

### III. RESULTS AND DISCUSSION

We measured the viscosity of our samples in the temperature interval 0–100 °C and extrapolated to lower-temperature values by a method due to

TABLE I. Viscosity parameters.

Sample	$10^3 \alpha$ (P)	$10^{-9} \beta$ ( $^{\circ}\text{K}^3$ )
glycerol	$1.80 \pm 0.04$	$0.2257 \pm 0.0005$
A	$1.91 \pm 0.06$	$0.2308 \pm 0.0008$
B	$1.73 \pm 0.09$	$0.2043 \pm 0.0015$
C	$1.78 \pm 0.07$	$0.1854 \pm 0.0011$

Litovitz.<sup>16,17</sup> He demonstrated that the viscosity of hydrogen-bonded solutions has a temperature dependence to the viscosity described by

$$\eta(T) = \alpha e^{\beta/T^3}, \quad (2)$$

where  $\alpha$  and  $\beta$  are constants which depend on the particular solution considered. Our data for  $\eta(T)$  fitted this relation quite well and the parameters obtained by a least-squares fit to our data are shown in Table I. A plot of our data based on Eq. (1) shows that the main effect of adding  $\text{FeCl}_2 \cdot 4\text{H}_2\text{O}$  to glycerol-water solutions was to raise the viscosity by about 15% over the entire temperature range studied.

The results of our diffusion measurements are summarized in Table II. These results represent diffusion runs ranging from 15 to 30 days using 0.55-mm-diam capillaries. The standard deviation in each value of the diffusion coefficient  $D$  reflects experimental errors from the counting geometry, measured time, and length of the capillaries. These errors do not include systematic errors such as a

TABLE II. Experimentally measured diffusion coefficient of samples A and C.

Anneal time (sec)	$T$ ( $^{\circ}\text{K}$ )	Capillaries No.	$L$ (cm)	Fractional activity drop	$D$ ( $\text{cm}^2/\text{sec}$ )
Sample A					
$1.99 \times 10^6$	$318 \pm 1$	1	1.86	0.17	$(3.82 \pm 0.38) \times 10^{-8}$
		2	2.23	0.13	$(3.55 \pm 0.36) \times 10^{-8}$
		3	2.21	0.14	$(3.64 \pm 0.54) \times 10^{-8}$
Average					$(3.67 \pm 0.25) \times 10^{-8}$
$1.55 \times 10^6$	$359 \pm 1$	1	1.95	0.40	$(2.94 \pm 0.07) \times 10^{-7}$
		2	1.94	0.41	$(3.20 \pm 0.07) \times 10^{-7}$
		3	2.23	0.36	$(3.33 \pm 0.10) \times 10^{-7}$
		4	2.43	0.33	$(3.17 \pm 0.10) \times 10^{-7}$
Average					$(3.16 \pm 0.04) \times 10^{-7}$
$7.78 \times 10^5$	$372.5 \pm 1.0$	1	2.19	0.37	$(6.61 \pm 0.12) \times 10^{-7}$
		2	1.97	0.41	$(6.63 \pm 0.20) \times 10^{-7}$
		3	2.40	0.35	$(7.20 \pm 0.20) \times 10^{-7}$
		4	2.10	0.41	$(7.31 \pm 0.30) \times 10^{-7}$
Average					$(6.94 \pm 0.11) \times 10^{-7}$
Sample C					
$1.64 \times 10^6$	$296 \pm 2$	1	2.17	0.13	$(3.91 \pm 0.39) \times 10^{-8}$
		2	2.36	0.12	$(3.65 \pm 0.37) \times 10^{-8}$
		3	2.20	0.10	$(2.57 \pm 0.26) \times 10^{-8}$
		4	2.43	0.11	$(3.31 \pm 0.30) \times 10^{-8}$
Average					$(3.36 \pm 0.21) \times 10^{-8}$

possible  $1^{\circ}\text{K}$  error in the temperature and about a 2% error in the measured average concentration of  $\text{Fe}^{59}$  after diffusion, caused by the washing out of the tracer solution from the capillary when dipped in the bath solution and during the run. Therefore, the errors quoted for  $D$  may be greater than shown in Table II. The magnitude of the 2% counting error will be significantly amplified for runs where the drop in activity is small. In the worst case ( $T = 318^{\circ}\text{K}$ ), we believe this effect is about 10%. It was found for sample C that the viscosity of the bath solution at the end of the experiment was about 40% smaller than its initial value. This decrease in viscosity can be explained by assuming that the sample picked up about 3% water during the diffusion run. Considering the hygroscopic character of the solution and the difficulties of keeping the diffusion container completely air tight for the long time interval over which the experiment was run, this result is not surprising. Thus, when comparing the  $D$  value with viscosity, via the Einstein-Stokes relation, we use an average value for the viscosity equal to 80% of the initial measured value at this temperature for sample C. The errors for this case are hard to estimate and might be quite large.

From the measured values of  $D$  and  $\eta$ , we were able to estimate the radius of the diffusing entity  $R$  by using the Einstein-Stokes relation<sup>18</sup>

$$D = kT/6\pi R\eta, \quad (3)$$

where  $D$  is the diffusivity and  $k$  is Boltzmann's constant. The results are shown in Table III, with and without the Robinson-Stokes<sup>19</sup> correction. The average radius of the diffusing particle with this correction is about  $3.9 \pm 0.4 \text{ \AA}$ , which is only slightly larger than the radius of a glycerol molecule ( $3 \text{ \AA}$ ) calculated from the molecular volume. Assuming the validity of the Einstein-Stokes relation for sample C, and taking for the viscosity 80% of its initial value, as pointed out earlier, the radius is found to be  $R = 4.28 \pm 0.65 \text{ \AA}$  after the Robinson-Stokes correction is applied. This is only 9% greater than the average value found for

TABLE III. Radii of diffusing entity from Einstein-Stokes relation for sample A. (Note: The systematic errors are such that all values should be regarded as only accurate to about 25% of the measured values even though the statistical errors calculated were much smaller in some cases.)

$T$ ( $^{\circ}\text{K}$ )	$R$ ( $\text{\AA}$ )	$R$ ( $\text{\AA}$ )
	calculated directly from Eq. (3)	with the Robinson-Stokes correction included
318	2.52	3.86
359	2.87	4.08
372.5	2.46	3.76

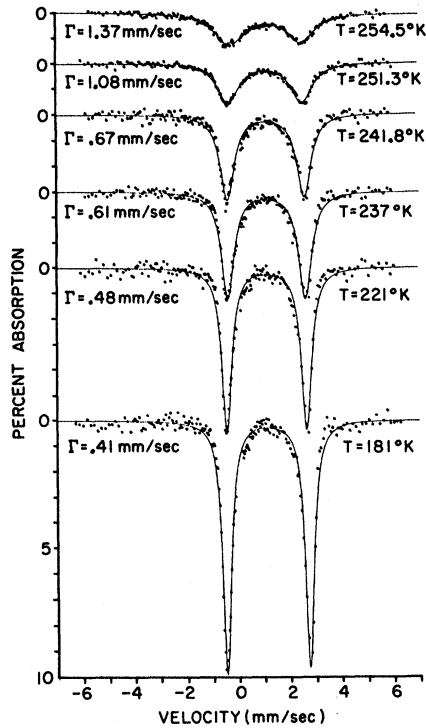


FIG. 1. Temperature dependence of Mössbauer spectra for sample A. Source was  $\text{Co}^{57}$  in palladium.

sample A, and it suggests that the radius of the diffusing entity is about the same for samples A, B, and C.

If we assume that the diffusion constant  $D$  is proportional to  $T/\eta$  in the region where diffusivity measurements were made, then we can fit  $D$  as a function of  $T$  with the aid of Eq. (2). The result is  $D = \gamma T e^{-\beta/T^3}$ , where

$$\gamma = (1.52 \pm 0.46) \times 10^{-7} \text{ cm}^2/\text{sec } ^\circ\text{K},$$

$$\beta = (0.232 \pm 0.009) \times 10^9 \text{ } ^\circ\text{K}^3.$$

It should be noted that the value of  $\beta$  is identical, within the experimental errors, to the value obtained from the direct viscosity measurements for sample A, as shown in Table II, supporting our assumption that  $D$  is proportional to  $T/\eta$  in the region where the diffusivity measurements were made.

A representative set of Mössbauer spectra for absorbers of type A, as a function of temperature, is shown in Fig. 1. The solid lines represent the fitted Lorentzian curves to the experimental data. The number of counts taken at each velocity ranged between  $2 \times 10^5$  and  $2 \times 10^6$ , depending on the percent effect at the maximum. Roughly, the number of counts accumulated was such that the statistical errors were about 5% of the absorption at the maximum. Systematic errors due to vibration, thermocouple calibration error, etc., were investigated and considered small compared to the statistical errors resulting from the limited number of counts at each velocity. Thus, we believe that the quoted standard errors are representative of the real experimental errors. Within the experimental errors, each curve in Fig. 1 is a symmetrical doublet with the same linewidth, area, and percent absorption for each peak. Although the data suggest some possible deviation from Lorentzian line shape, the effects are small and believed to be within the experimental errors. The best estimate of the Mössbauer parameters with their standard errors are summarized in Tables IV–VI, where  $\Gamma$  is the average value of the linewidth of the two peaks,  $A_T$  is the total area under the curve,  $Q_S = v_1 - v_2$  is the quadrupole splitting, and  $I_S = \frac{1}{2}(v_1 + v_2)$  is the isomer shift relative to palladium. The spectra for each of the three solutions can be identified as due to  $\text{Fe}^{2+}$  ions from the  $I_S (\approx 1.1 \text{ mm/sec})$  and  $Q_S (\approx 3$

TABLE IV. Experimentally measured Mössbauer parameters for sample A.

$T$ (°K)	$\Gamma$ (mm/sec)	$A_T$	$V_1$ (mm/sec)	$V_2$ (mm/sec)	$Q_S$ (mm/sec)	$I_S$ (mm/sec)
122.5	$0.410 \pm 0.007$	$0.1664 \pm 0.0020$	$2.775 \pm 0.003$	$-0.482 \pm 0.002$	$3.257 \pm 0.004$	$1.147 \pm 0.002$
160.2	$0.409 \pm 0.007$	$0.1405 \pm 0.0017$	$2.737 \pm 0.003$	$-0.479 \pm 0.003$	$3.216 \pm 0.004$	$1.129 \pm 0.002$
181.0	$0.411 \pm 0.008$	$0.1255 \pm 0.0018$	$2.712 \pm 0.004$	$-0.483 \pm 0.003$	$3.195 \pm 0.005$	$1.115 \pm 0.003$
193.0	$0.422 \pm 0.009$	$0.1215 \pm 0.0018$	$2.700 \pm 0.004$	$-0.480 \pm 0.003$	$3.180 \pm 0.005$	$1.110 \pm 0.003$
211.3	$0.461 \pm 0.011$	$0.1060 \pm 0.0020$	$2.657 \pm 0.006$	$-0.460 \pm 0.004$	$3.117 \pm 0.007$	$1.099 \pm 0.003$
221.0	$0.478 \pm 0.012$	$0.0957 \pm 0.0018$	$2.629 \pm 0.006$	$-0.454 \pm 0.005$	$3.083 \pm 0.008$	$1.088 \pm 0.004$
226.5	$0.517 \pm 0.013$	$0.0911 \pm 0.0018$	$2.614 \pm 0.007$	$-0.444 \pm 0.005$	$3.058 \pm 0.009$	$1.085 \pm 0.005$
232.5	$0.544 \pm 0.015$	$0.0809 \pm 0.0018$	$2.587 \pm 0.008$	$-0.439 \pm 0.006$	$3.026 \pm 0.010$	$1.074 \pm 0.005$
237.0	$0.607 \pm 0.015$	$0.0795 \pm 0.0016$	$2.571 \pm 0.007$	$-0.426 \pm 0.006$	$2.997 \pm 0.009$	$1.073 \pm 0.005$
241.8	$0.671 \pm 0.018$	$0.0691 \pm 0.0018$	$2.551 \pm 0.009$	$-0.419 \pm 0.007$	$2.970 \pm 0.011$	$1.066 \pm 0.006$
245.5	$0.837 \pm 0.026$	$0.0661 \pm 0.0018$	$2.513 \pm 0.012$	$-0.385 \pm 0.011$	$2.898 \pm 0.016$	$1.064 \pm 0.008$
249.5	$0.986 \pm 0.023$	$0.0595 \pm 0.0013$	$2.513 \pm 0.010$	$-0.365 \pm 0.009$	$2.878 \pm 0.013$	$1.074 \pm 0.007$
251.3	$1.075 \pm 0.023$	$0.0542 \pm 0.0010$	$2.485 \pm 0.010$	$-0.342 \pm 0.009$	$2.827 \pm 0.013$	$1.072 \pm 0.007$
254.5	$1.365 \pm 0.032$	$0.0497 \pm 0.0011$	$2.444 \pm 0.014$	$-0.296 \pm 0.012$	$2.740 \pm 0.018$	$1.074 \pm 0.009$

TABLE V. Experimentally measured Mössbauer parameters for sample B.

$T$ (°K)	$\Gamma$ (mm/sec)	$A_T$	$V_1$ (mm/sec)	$V_2$ (mm/sec)	$Q_S$ (mm/sec)	$I_S$ (mm/sec)
120.0	0.383 ± 0.006	0.1344 ± 0.0016	2.797 ± 0.003	-0.470 ± 0.002	3.267 ± 0.004	1.164 ± 0.002
152.5	0.398 ± 0.007	0.1205 ± 0.0016	2.768 ± 0.003	-0.474 ± 0.003	3.242 ± 0.004	1.147 ± 0.002
178.5	0.409 ± 0.007	0.1068 ± 0.0014	2.729 ± 0.004	-0.476 ± 0.003	3.205 ± 0.005	1.127 ± 0.003
197.5	0.423 ± 0.009	0.0946 ± 0.0015	2.704 ± 0.004	-0.470 ± 0.003	3.174 ± 0.005	1.117 ± 0.003
209.5	0.446 ± 0.009	0.0851 ± 0.0013	2.682 ± 0.005	-0.458 ± 0.003	3.140 ± 0.006	1.112 ± 0.003
219.5	0.488 ± 0.010	0.0787 ± 0.0012	2.642 ± 0.005	-0.446 ± 0.004	3.088 ± 0.006	1.098 ± 0.003
225.0	0.514 ± 0.011	0.0722 ± 0.0012	2.636 ± 0.006	-0.437 ± 0.005	3.073 ± 0.008	1.100 ± 0.004
230.0	0.571 ± 0.015	0.0641 ± 0.0013	2.628 ± 0.007	-0.423 ± 0.005	3.051 ± 0.009	1.102 ± 0.005
233.5	0.602 ± 0.016	0.0592 ± 0.0013	2.585 ± 0.008	-0.413 ± 0.006	2.998 ± 0.009	1.086 ± 0.005
236.5	0.693 ± 0.015	0.0548 ± 0.0010	2.580 ± 0.007	-0.407 ± 0.006	2.987 ± 0.009	1.087 ± 0.005
240.0	0.798 ± 0.018	0.0516 ± 0.0010	2.563 ± 0.008	-0.391 ± 0.008	2.954 ± 0.011	1.086 ± 0.006
243.4	1.047 ± 0.028	0.0451 ± 0.0011	2.530 ± 0.013	-0.355 ± 0.011	2.885 ± 0.017	1.088 ± 0.008
246.0	1.255 ± 0.039	0.0397 ± 0.0011	2.520 ± 0.019	-0.349 ± 0.014	2.869 ± 0.011	1.086 ± 0.011
249.0	1.553 ± 0.056	0.0369 ± 0.0013	2.449 ± 0.016	-0.289 ± 0.019	2.738 ± 0.025	1.080 ± 0.012
250.0	1.64 ± 0.12	0.0321 ± 0.0021	2.488 ± 0.054	-0.291 ± 0.038	2.779 ± 0.066	1.099 ± 0.033

mm/sec), since the typical ferrous ion has an  $I_S$  between 1.0 and 1.5 mm/sec, with  $Q_S$  between 2–4 mm/sec. The data for samples B and C were of the same quality,<sup>6</sup> and a Co<sup>57</sup>-doped palladium source was used in all of the experiments.

From the measured linewidths given in Table IV–VI we can calculate the incremental broadening of the Mössbauer line,  $\Delta\epsilon = \Gamma - \Gamma_M$ . The width of our line without diffusion,  $\Gamma_M$ , was taken as an average of the measured low-temperature widths below the glass-liquid transition temperatures of 185, 175, and 170 °K for samples A, B, and C, respectively. The values of  $\Gamma_M$  in mm/sec are 0.409 ± 0.004, 0.391 ± 0.005, and 0.385 ± 0.005 for samples A, B, and C, respectively. In Table VII, we show the results of this calculation where the relative broadening  $\Delta\epsilon/\Gamma_N$  and the extrapolated viscosities are given for each temperature where the Mössbauer spectrum was observed. At low temperatures the error in the broadening is quite

large, because  $\Delta\epsilon$  is the difference in two linewidths which are nearly of the same magnitude. It should be mentioned that the subtracted minimum width  $\Gamma_M$  will in part contain a term involving the “finite thickness” correction, which will decrease as the probability of recoil-free absorption decreases and as the temperature increases. We have not included this correction, although we estimate that it does not change sufficiently to significantly alter the uncorrected incremental broadenings given in Table VII.

Since the Singwi–Sjölander<sup>1</sup> theory predicts that the broadening of the Mössbauer line should be proportional to the diffusivity, and since the Einstein–Stokes relation predicts a diffusivity proportional to  $T/\eta$ , we might expect a plot of  $\Delta\epsilon/\Gamma_N$  vs  $T/\eta$  to be linear, as was apparently confirmed by Craig and Sutin.<sup>5</sup> Our results are shown in Fig. 2 and it is clear that a simple linear relation does not give a satisfactory representation to our data.

TABLE VI. Experimentally measured Mössbauer parameters for sample C.

$T$ (°K)	$\Gamma$ (mm/sec)	$A_T$	$V_1$ (mm/sec)	$V_2$ (mm/sec)	$Q_S$ (mm/sec)	$I_S$ (mm/sec)
133.0	0.386 ± 0.007	0.1183 ± 0.0016	2.791 ± 0.003	-0.470 ± 0.003	3.261 ± 0.004	1.161 ± 0.002
152.5	0.384 ± 0.007	0.1094 ± 0.0013	2.786 ± 0.003	-0.472 ± 0.002	3.258 ± 0.004	1.157 ± 0.002
179.5	0.408 ± 0.007	0.0972 ± 0.0013	2.752 ± 0.004	-0.468 ± 0.003	3.220 ± 0.004	1.142 ± 0.003
196.0	0.429 ± 0.010	0.0881 ± 0.0014	2.718 ± 0.005	-0.461 ± 0.004	3.179 ± 0.006	1.129 ± 0.003
210.5	0.464 ± 0.011	0.0763 ± 0.0014	2.684 ± 0.006	-0.445 ± 0.004	3.129 ± 0.008	1.120 ± 0.004
221.3	0.513 ± 0.014	0.0647 ± 0.0014	2.648 ± 0.007	-0.430 ± 0.005	3.078 ± 0.009	1.109 ± 0.005
224.0	0.526 ± 0.013	0.0616 ± 0.0012	2.634 ± 0.007	-0.423 ± 0.005	3.057 ± 0.009	1.106 ± 0.005
226.8	0.561 ± 0.016	0.0550 ± 0.0012	2.625 ± 0.008	-0.421 ± 0.006	3.046 ± 0.009	1.102 ± 0.005
230.7	0.648 ± 0.018	0.0496 ± 0.0011	2.600 ± 0.009	-0.408 ± 0.007	3.008 ± 0.011	1.096 ± 0.006
233.0	0.732 ± 0.023	0.0497 ± 0.0014	2.600 ± 0.011	-0.388 ± 0.009	2.988 ± 0.014	1.106 ± 0.007
237.0	0.971 ± 0.026	0.0444 ± 0.0011	2.548 ± 0.013	-0.356 ± 0.011	2.904 ± 0.017	1.096 ± 0.009
240.0	1.203 ± 0.030	0.0423 ± 0.0009	2.535 ± 0.014	-0.343 ± 0.010	2.878 ± 0.017	1.096 ± 0.009
242.0	1.388 ± 0.049	0.0365 ± 0.0011	2.531 ± 0.021	-0.300 ± 0.018	2.831 ± 0.028	1.116 ± 0.014

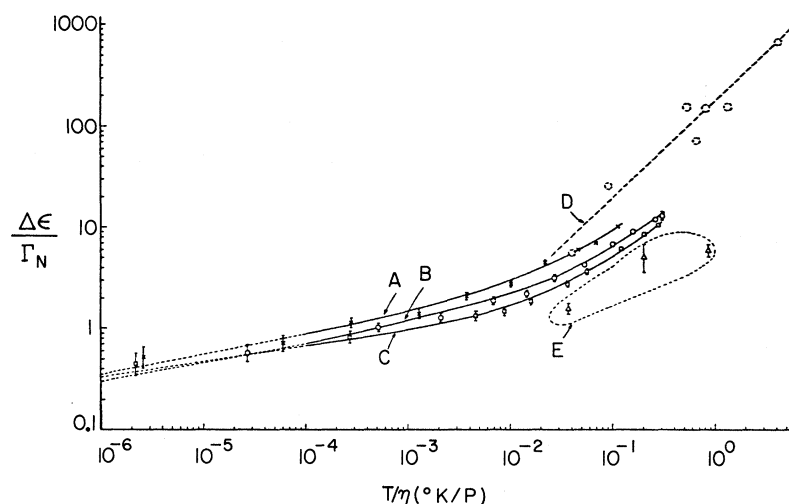


FIG. 2. Dependence of diffusional broadening on viscosity. Curve D is a rough representation of Craig and Sutin's data (Ref. 5) reprocessed to correspond to our notation and E represents data by Champeney and Woodhams (Ref. 9). Since case E represent the results of scattering experiments from pure glycerol, we would not expect these results to be directly comparable to our own, although the similarity in slope in the overlapping temperature interval is significant.

Our results are in reasonable agreement with those of Champeney and Woodhams,<sup>9</sup> considering that they were measuring the scattering from pure glycerol. The temperature dependence of the broadening that they observed is comparable with that which we find in the region of overlap. This indicates that the  $\text{Fe}^{2+}$  diffusion is indeed directly related to the glycerol diffusion in this temperature interval. Because of the increasing dominance of the continuous mechanism at higher temperatures, our data will be parallel, although somewhat displaced from that of Craig and Sutin, if we project into the region  $T/\eta \gtrsim 1$  by using the equation and parameters given in Table VIII. For our experiment the resonance dip was only about  $\frac{1}{2}\%$  when the broadening was of order  $10\Gamma_N$ , thus putting an upper limit to the temperature range of our measurements. Hence, we believe that the simple  $T/\eta$  dependence to the line broadening observed by Craig and Sutin was caused

by a lack of sufficiently low temperature data and the rough accuracy of their early experiment. The difference in their calculated particle radius (0.7 Å) and ours (2.6 Å) is indicative of the displacement in their curve (Fig. 2 D) and our curve A at  $T/\eta = 1$ .

It should also be noted that curves A, B, and C in Fig. 2 are clearly distinguished. If the simple Einstein-Stokes relation and the Singwi-Sjölander theory were both adequate to describe our system, we should expect these three curves to be superimposed in a single straight line.

In Fig. 3, we have plotted the broadening of the Mössbauer line as a function of  $1/T$ . In the low-temperature region the curves approach an Arrhenius relation. If we assume that the diffusion consists of two distinct mechanisms, which are statistically independent, then we would expect  $D = D_1 + D_2$ . We are able to give a very satisfactory fit

TABLE VII. Relative diffusional broadening and viscosity as function of  $T$ .

Sample A			Sample B			Sample C		
$T$ (°K)	$\Delta\epsilon/\Gamma_N$	$\eta^a$ (P)	$T$ (°K)	$\Delta\epsilon/\Gamma_N$	$\eta^a$ (P)	$T$ (°K)	$\Delta\epsilon/\Gamma_N$	$\eta^a$ (P)
193.0	$0.13 \pm 0.10$	$1.66 \times 10^{11}$	178.5	$0.18 \pm 0.09$	$6.85 \times 10^{12}$	179.5	$0.24 \pm 0.09$	$1.49 \times 10^{11}$
211.3	$0.53 \pm 0.12$	$8.11 \times 10^7$	197.5	$0.33 \pm 0.11$	$5.66 \times 10^8$	196.0	$0.45 \pm 0.11$	$8.80 \times 10^7$
221.0	$0.71 \pm 0.13$	$3.70 \times 10^6$	209.5	$0.57 \pm 0.11$	$7.69 \times 10^6$	210.5	$0.81 \pm 0.12$	$7.69 \times 10^5$
226.5	$1.11 \pm 0.14$	$8.08 \times 10^5$	219.5	$1.00 \pm 0.11$	$4.25 \times 10^5$	221.3	$1.32 \pm 0.15$	$4.80 \times 10^4$
232.5	$1.39 \pm 0.16$	$1.80 \times 10^5$	225.0	$1.26 \pm 0.12$	$1.06 \times 10^5$	224.0	$1.45 \pm 0.14$	$2.59 \times 10^4$
237.0	$2.03 \pm 0.16$	$6.44 \times 10^4$	230.0	$1.85 \pm 0.16$	$3.40 \times 10^4$	226.8	$1.81 \pm 0.17$	$1.42 \times 10^4$
241.8	$2.69 \pm 0.19$	$2.36 \times 10^4$	233.5	$2.17 \pm 0.17$	$1.62 \times 10^4$	230.7	$2.70 \pm 0.19$	$6.46 \times 10^3$
245.5	$4.40 \pm 0.27$	$1.13 \times 10^4$	236.5	$3.10 \pm 0.16$	$8.79 \times 10^3$	233.0	$3.57 \pm 0.24$	$4.14 \times 10^3$
249.5	$5.93 \pm 0.24$	$5.43 \times 10^3$	240.0	$4.18 \pm 0.19$	$4.55 \times 10^3$	237.0	$6.02 \pm 0.27$	$1.99 \times 10^3$
251.3	$6.84 \pm 0.24$	$3.68 \times 10^3$	243.4	$6.74 \pm 0.29$	$2.45 \times 10^3$	240.0	$8.41 \pm 0.31$	$1.19 \times 10^3$
254.5	$9.83 \pm 0.33$	$2.29 \times 10^2$	246.0	$8.88 \pm 0.40$	$1.58 \times 10^3$	242.0	$10.31 \pm 0.51$	$8.54 \times 10^2$
			249.0	$11.94 \pm 0.58$	$9.65 \times 10^2$			
			250.0	$12.8 \pm 1.2$	$8.25 \times 10^2$			

<sup>a</sup>These values are extrapolated from our experimental values.

TABLE VIII. Broadening parameters for the relation  $\Delta\epsilon/\Gamma_N = A_1 T e^{-\beta/T^3} + A_2 e^{-E/kT}$ .

Sample	$10^{-4}A_1$ ( $^{\circ}\text{K}^{-1}$ )	$10^{-5}A_2$	$E$ (eV)
A	$2.58 \pm 0.23$	$4.50 \pm 5.52$	$0.252 \pm 0.025$
B	$1.65 \pm 0.10$	$2.40 \pm 3.38$	$0.234 \pm 0.028$
C	$1.52 \pm 0.08$	$0.13 \pm 0.19$	$0.176 \pm 0.029$

to our data, as evidenced by the solid lines shown in Fig. 3, by assuming that  $D_1$  is due to continuous diffusion, so that

$$D_1 \propto \Delta\epsilon_1/\Gamma_N = A_1 T e^{-\beta/T^3},$$

where the latter expression is derived from the Litovitz<sup>16</sup> Eq. (2) and  $D_2$  is due to an activated diffusion process and is described by an Arrhenius temperature dependence, i. e.,

$$D_2 \propto \Delta\epsilon_2/\Gamma_N = A_2 e^{-E/kT}.$$

The three-parameter least-squares fit to the data, with appropriate weighting factors to account for the difference in error bars in the data, gives the values of  $A_1$ ,  $A_2$ , and  $E$  shown in Table VIII. It should be emphasized that  $\beta$  was not allowed to vary in this calculation, but was taken directly from the curves fitted to the measured viscosity, i. e., the values used were the same as shown in Table I.

The fit to the data is excellent and the correctness of this interpretation is augmented by a comparison with the results of Larsson and Dahlborg,<sup>20</sup> who measured proton diffusion in glycerol by means of neutron-scattering experiments. Although they fitted their data to a sum of Arrhenius relations, the slopes in the low- and high-temperature regions are quite similar to the values we obtain by our Mössbauer studies. The difference in the temperature of the bend in our curve and theirs could be explained by the fact that the diffusing entity in our

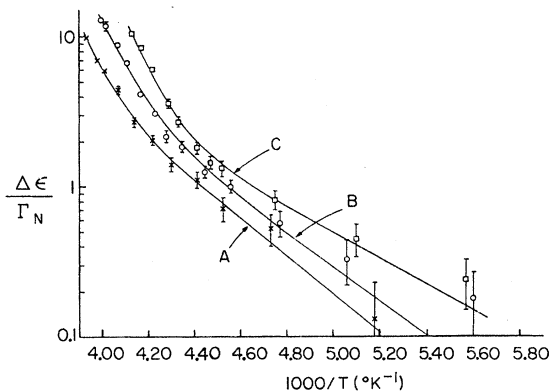


FIG. 3. Temperature dependence of the diffusional broadening for samples A, B, and C.

case contains  $\text{Fe}^{57}$ . This discrepancy will be reduced in any event if we plot  $\ln D$  vs  $1/T$  from our data. This cannot be done, however, as insufficient diffusivity data are available to determine  $\sigma$  for the jump part of the diffusivity, which we noted in the discussion of Eq. (1) is much smaller in the sudden-jump limit. The difference in the magnitude of the  $D$  values cannot be explained so easily, although the mass difference would account for some of this discrepancy.

The present measurements afford an opportunity to measure  $\sigma$  in the continuous-diffusion limit. We wish to compare  $\Delta\epsilon_1$  with the measured diffusivity in the high-temperature region, where the continuous component to the diffusivity is dominant, with the predictions of the Singwi-Sjölander theory in the continuous diffusion limit  $\tau_1 \gg \tau_0$ . We can do this by extrapolating  $\Delta\epsilon_1/\Gamma_N$  to the temperature where we made tracer measurements of the diffusivity by means of the tracer-capillary technique, and then calculating  $\sigma$  at those temperatures from Eq. (1). This procedure gives the values shown in Table IX. The average value of  $\sigma = 2.24 \pm 0.13$  is in excellent agreement with the theoretically expected value  $\sigma = 2.0$  since the error limit does not include systematic errors in the diffusivity measurements.

We were not able to get sufficient tracer-diffusion data for samples of type B and C to permit this same type of comparison. If we do use the values of  $D$  measured for sample C at 296  $^{\circ}\text{K}$ , we can show that to within the accuracy that we know the average viscosity, we may write, for fixed temperature,

$$D_C/D_A = \eta_A/\eta_C, \quad (4)$$

which implies that the forms of the Einstein-Stokes relation holds in this temperature region, and that the effective radius  $R$  of the diffusing entity is essentially constant. Assuming the constancy of the radius of the diffusing entity, Eq. (1), and the analogous relation for sample type B, we find  $\sigma \approx 1.30$  and  $1.23$  for samples B and C, respectively. If we use the directly measured  $D$  value for sample C (Table III), we obtain  $\sigma \approx 1.35$ . The small difference between the two values ( $1.35$  vs  $1.23$ ) again indicates that the assumption of a constant radius for the diffusing entity is valid to within about 10%. Although the statistical errors show a small deviation from the value in the Singwi-Sjölander theory,

TABLE IX. Calculated values of  $\sigma$  for sample A.

$T$ ( $^{\circ}\text{K}$ )	$\sigma$
318	$2.16 \pm 0.24$
359	$2.54 \pm 0.23$
372.5	$2.02 \pm 0.18$

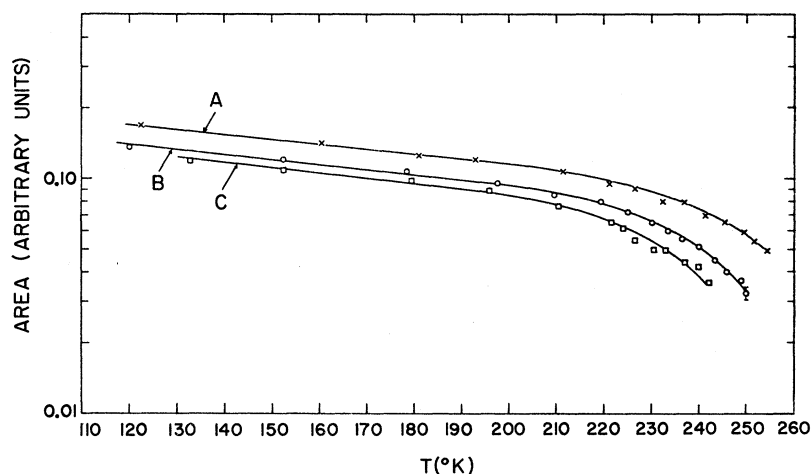


FIG. 4. Temperature dependence of the area under Mössbauer resonance for samples A, B, and C.

we think that these statistical errors are smaller than the real errors for cases B and C because the error in diffusivity probably is greater than shown in Table II. We regard the excellent agreement with theory for sample A, for which we had the best diffusion data, as strong evidence that this continuous limit of the theory is a satisfactory description of the continuous part of the diffusion motion in glycerol. Even taking into account the values of  $\sigma$  for samples B and C, we still find a value of  $\sigma$  in reasonable harmony with theory. The mean value of  $\sigma$  for all three samples is 1.6, which is only 20% below the expected value of 2.0. We regard this as excellent agreement in view of the uncertainties in determining the diffusion coefficient for samples B and C.

We have found that in the temperature region where diffusion occurs there is a very rapid falloff in the recoil-free fraction. Neglecting changes in the "finite-thickness" correction, the recoil-free fraction is proportional to the area under the Mössbauer resonance-absorption curve. A plot of  $\ln A_T$  vs  $T$  is shown in Fig. 4 for our samples A, B, and C. The curves follow the expected linear dependence predicted by the Debye model below the glass-liquid transition temperature until we reach a temperature of about 200 °K, where diffusion effects are observed. In this region we find that the falloff in  $\ln f$  is much more rapid, and the effect is similar to earlier<sup>3</sup> results for Fe<sup>57</sup> in Cu and Au.

In the linear region, the values of the Mössbauer characteristic temperature were calculated to be 170, 172, and 177 °K for samples A, B, and C, respectively. The absolute errors are probably within about 10 °K, and the relative errors are of order 2 °K. Errors from the changes in finite-thickness correction and the use of the linear approximation have not been included. These values are comparable with the Mössbauer characteristic temperature for glycerol found from neutron-

scattering experiments<sup>21</sup> ( $\theta_M \approx 150$  °K).

Jensen<sup>10</sup> has recently proposed a phenomenological theory, which indicates that the broadening of the Mössbauer line should be proportional to  $\ln f$  even though both  $\Delta\epsilon$  and  $f$  have a complicated temperature dependence. A plot of  $\Delta\epsilon/\Gamma_N$  vs  $-\ln f$  is given in Fig. 5. The data can be represented reasonably well by two straight lines in the low- and high-temperature regions with intercepts at 235, 233, and 227 °K for samples A, B, and C, respectively. The superposition of curves (a) and (b) at high temperatures and (b) and (c) at low temperatures is probably statistically fortuitous. The linearity between the diffusion broadening and  $\ln f$  would imply from Jensen's analysis that the vibratory and jumping motions are not independent. The possibility of an alternative explanation of the rapid falloff of  $\ln f$  in the temperature region where diffusion is occurring, such as anharmonic effects,<sup>22</sup> cannot be ruled out, particularly in view of the

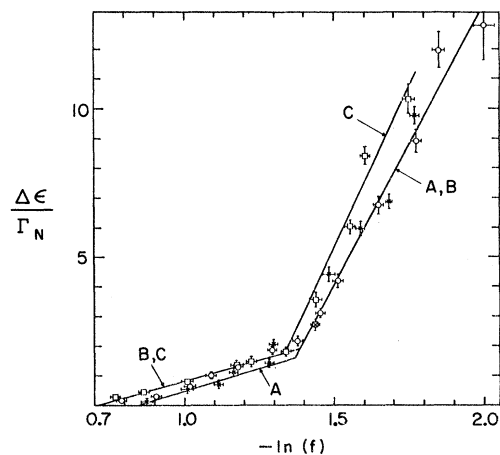


FIG. 5. Correlation between Mössbauer line broadening and recoil-free fraction.

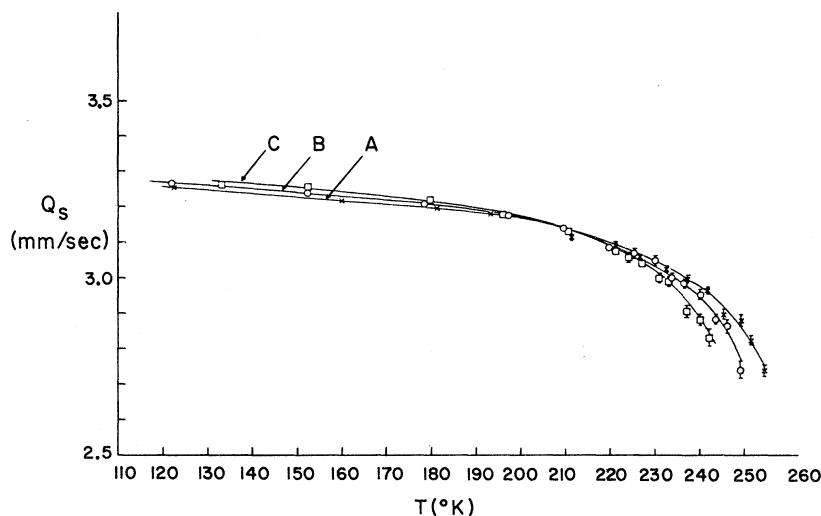


FIG. 6. Temperature dependence of the quadrupole splitting for samples A, B, and C.

limited precision of the quantities measured in the plot of Fig. 5.

In Fig. 6 we show a plot of the quadrupole splitting ( $Q_s$ ) as a function of temperature. Again we see a very rapid falloff in the temperature interval above the glass-liquid transition temperature where diffusion-broadening effects were observed. This suggested that a plot of  $\Delta\epsilon/\Gamma_N$  vs  $Q_s$  might also yield a linear relation, which is well confirmed in Fig. 7. Again the turning points in the linear relations 233, 232, and 225 °K for samples A, B, and C, respectively, are comparable to those from the curve in Fig. 5. We fitted

$$\Delta\epsilon/\Gamma_N = B_1 - B_2 [Q_s(T)/Q_s(T_0)]$$

with our general least-squares program, and the parameters  $B_1$  and  $B_2$  are given in Table X. The small error limits are indicative of the high degree of linearity in both the low- and high-temperature regions.

Although the temperature dependence of the quadrupole splitting for  $\text{Fe}^{2+}$  in ionic salts has been studied by Ingalls,<sup>23</sup> his analysis does not seem adequate to explain our results, which deal with the same ferrous ion in glycerol. Ingalls considered the splitting of the energy levels of the ferrous ion caused by the crystalline field and assumed that the thermal transition times between levels

( $10^{-9}$ – $10^{-11}$  sec) are smaller than the quadrupole-splitting precession time ( $\sim 10^{-8}$  sec). Based on this assumption, the quadrupole splitting is expressed as a function of temperature through a Boltzmann distribution for occupancy of the split levels. His results predict, for  $\text{FeCl}_2 \cdot 4\text{H}_2\text{O}$ , a decreasing in the quadrupole splitting of  $\sim 10\%$  for an increasing in temperature from about 80 to 330 °K and agree with the experimental results. Below the glass transition temperature we also observed a similar gradual reduction in the quadrupole splitting, which could probably be explained by Ingalls's approach. In our study, however, where the same salt was used, we have observed a sudden 12% decrease in the quadrupole splitting over only a 50 °K increase in temperature in the region where diffusion occurred. This strongly supports the view that the diffusive motions are contributing to the rapid falloff in the quadrupole splitting.

A simple explanation for this observation can

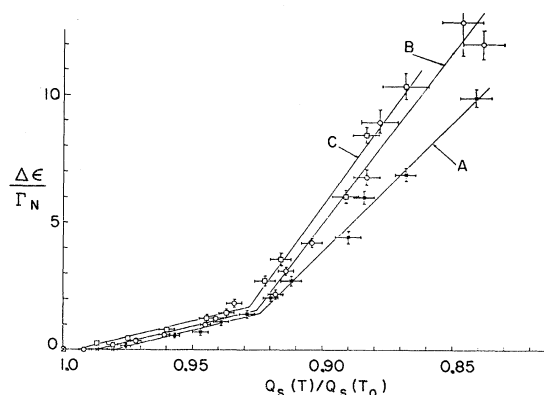


FIG. 7. Correlation between Mössbauer line broadening and quadrupole splitting for samples A, B, and C.

TABLE X. Parameters fit to Fig. 5.

Sample	$B_1$		$B_2$	
	Low-temp. region	High-temp. region	Low-temp. region	High-temp. region
A	$26.4 \pm 2.7$	$100.3 \pm 7.3$	$25.8 \pm 2.6$	$94.0 \pm 6.4$
B	$25.4 \pm 2.4$	$134.6 \pm 6.4$	$25.1 \pm 2.3$	$126.1 \pm 5.6$
C	$24.9 \pm 1.4$	$138.3 \pm 1.2$	$24.7 \pm 1.3$	$130.1 \pm 10.8$

be given if we assume that the time-average electric field gradient diminishes proportionally to the diffusivity or rate of jumping, i. e., the electric field gradient reduces in proportion to the jumping frequency, or  $\Delta\epsilon/\Gamma_N$ . The change in slope again reflects, by this analysis, a change in the dominant diffusion mechanism from sudden jump to continuous as we go from low to high temperatures.

It should be mentioned that, in general, the problem of calculating time-dependent relaxation effects of hyperfine structure is very involved.<sup>24,25</sup> For the present case, however, where the hyperfine splitting is large compared to the natural line-

width of the isomeric level, it appears that the effects of diffusion on the quadrupole splitting is quite simple. A more detailed theoretical analysis, however, would be desirable.

#### ACKNOWLEDGMENTS

We would like to thank Professor C. A. Angell and E. Sare for aid in chemistry problems in the early stages of this work, Professor P. H. Keesom for helpful criticism of the work, and Professor D. St. P. Bunbury for valuable correspondence on this subject.

\*Work supported by the National Science Foundation, the Atomic Energy Commission, and the Advanced Research Projects Agency (IDL Program, No. DAHC-0213), and based on the Ph.D. thesis research of Abras. One of us (A. A.) would like to thank the Rockefeller Foundation for fellowship support towards this work.

†Present address: Instituto Ciências Exatas, Universidade Federal De Minas Gerais, Cidade Universitária-Pampulha, Belo Horizonte, M. G. Brazil.

<sup>1</sup>K. S. Singwi and A. Sjölander, *Phys. Rev.* **120**, 1093 (1960).

<sup>2</sup>L. Van Hove, *Phys. Rev.* **95**, 249 (1954).

<sup>3</sup>R. C. Knauer and J. G. Mullen, *Phys. Rev.* **174**, 711 (1968); J. G. Mullen and R. C. Knauer, in *Mössbauer Effect Methodology*, edited by I. J. Gruverman (Plenum, New York, 1969), Vol. 5, pp. 197-208.

<sup>4</sup>D. St. P. Bunbury, J. A. Elliot, H. E. Hall, and J. M. Williams, *Phys. Letters* **6**, 34 (1963).

<sup>5</sup>P. P. Craig and N. Sutin, *Phys. Rev. Letters* **11**, 460 (1963).

<sup>6</sup>A. Abras, Ph.D. thesis (Purdue University, 1972), (unpublished).

<sup>7</sup>R. C. Knauer, *Phys. Rev. B* **3**, 3 (1971); **3**, 567 (1971).

<sup>8</sup>M. A. Krivoglaz and S. P. Repetskii, *Fiz. Metal. i Metalloved.* **32**, No. 5, 899 (1971).

<sup>9</sup>D. C. Champeney and P. W. D. Woodhams, *Proc. Phys. Soc. (London)* **1**, 620 (1968).

<sup>10</sup>J. H. Jensen, *Phys. Kondensierten Materie* **13**, 273 (1971).

<sup>11</sup>J. G. Mullen, *Atomic Transport in Solids and Liquids* (Zeitschrift für Naturforschung, Tuebingen, Germany, 1971), p. 395.

<sup>12</sup>R. C. Knauer and J. G. Mullen, *Rev. Sci. Instr.* **38**, 1624 (1967).

<sup>13</sup>J. H. Wang, *J. Am. Chem. Soc.* **73**, 510 (1951).

<sup>14</sup>R. E. Hoffman, *J. Chem. Phys.* **20**, 1567 (1952).

<sup>15</sup>R. Mills and J. W. Kennedy, *J. Am. Chem. Soc.* **75**, 5696 (1953).

<sup>16</sup>T. A. Litovitz, *J. Chem. Phys.* **20**, 1088 (1952).

<sup>17</sup>R. Piccirelli and T. A. Litovitz, *J. Acoust. Soc. Am.* **29**, 1009 (1957).

<sup>18</sup>J. Frenkel, *Kinematic Theory of Liquids* (Clarendon, Oxford, England, 1946), p. 193.

<sup>19</sup>R. A. Robinson and R. H. Stokes, *Electrolyte Solutions* (Academic, New York, 1955), pp. 118-121.

<sup>20</sup>K. E. Larsson and V. Dahlborg, *Physica* **30**, 1561 (1971).

<sup>21</sup>K. E. Larsson and K. S. Singwi, *Phys. Letters* **3**, 145 (1962).

<sup>22</sup>K. N. Pathak and B. Deo, *Physica* **35**, 167 (1967).

<sup>23</sup>R. Ingalls, *Phys. Rev.* **133**, A787 (1964).

<sup>24</sup>M. J. Clouser and M. Blume, *Phys. Rev. B* **3**, 3 (1971); **3**, 583 (1971).

<sup>25</sup>M. A. Krivoglaz and S. P. Repetskii, *Fiz. Metal. i Metalloved.* **32**, No. 6, 1158 (1971).